A two-component model of phytoplankton absorption in the open ocean: Theory and applications

E. Devred,[1,2] S. Sathyendranath,[1,2] V. Stuart,[1,2] H. Maass,[2] O. Ulloa,[3] and T. Platt[2]

Received 16 January 2005; revised 1 November 2005; accepted 10 December 2005; published 23 March 2006.

[1] The two-population absorption model of Sathyendranath et al. is extended to retrieve the specific absorption coefficients (absorption per unit concentration of chlorophyll-*a*) of the component populations of phytoplankton. The model relates the absorption coefficient of phytoplankton to chlorophyll-*a* concentration, assuming that the assemblages of phytoplankton comprise mixtures of two populations whose proportions vary as the total concentration of cells changes. The model is applied to in situ data collected from six regions during 34 cruises. The model compares well with earlier models of phytoplankton absorption but brings the additional advantage of parameters that have clear bio-optical and biological interpretation. Size structure of the phytoplankton populations was inferred from the values of the specific absorption coefficients. The results are consistent with pigment analyses performed on the same samples. Seasonal analysis of data from the northwest Atlantic, southeast Pacific, and the Arabian Sea showed significant changes in the spectral form and magnitude of the specific absorption coefficients of small- and large-celled populations, which appear to be related to changes in species composition. The model serves thus as an optical tool to explore the large-scale biogeography of phytoplankton.

Citation: Devred, E., S. Sathyendranath, V. Stuart, H. Maass, O. Ulloa, and T. Platt (2006), A two-component model of phytoplankton absorption in the open ocean: Theory and applications, *J. Geophys. Res.*, *111*, C03011, doi:10.1029/2005JC002880.

1. Introduction

[2] Absorption coefficient of phytoplankton from the oceanic environment is a nonlinear function of the dominant phytoplankton pigment, chlorophyll-*a* [*Bricaud et al.*, 1995; *Cleveland*, 1995]. This nonlinearity results from changes in the size structure and pigment complement of the phytoplankton population [*Prieur and Sathyendranath*, 1981; *Hoepffner and Sathyendranath*, 1991; *Fujiki and Taguchi*, 2002; *Lohrenz et al.*, 2003] as one moves from oligotrophic (low-chlorophyll) to eutrophic (high-chlorophyll) waters [*Hoepffner and Sathyendranath*, 1992, 1993; *Claustre*, 1994; *Ciotti et al.*, 1999; *Sathyendranath et al.*, 2005]. Typically, the oligotrophic waters are dominated by small cells that harvest light with higher efficiency [*Duysens*, 1956] than large cells, which tend to dominate in eutrophic environments.

[3] Several authors have expressed phytoplankton absorption coefficient as a function of chlorophyll concentration [*Prieur and Sathyendranath*, 1981; *Morel*, 1991; *Cleveland*, 1995; *Bricaud et al.*, 1995, 1998] using a simple power law of the type $a_p(\lambda) = A(\lambda)C^{-B(\lambda)}$ where λ is wavelength and parameters A and B are optimized so that the function fits the observations. Michaelis-Menten-type equations have also been used in this context [*Sathyendranath and Platt*, 1988; *Lutz et al.*, 1996; *Sathyendranath et al.*, 2001]. Such models are good empirical descriptions of the observed nonlinear relationship between absorption and pigment concentrations. However, it is difficult to justify the choice of such functions based on biological or optical considerations. Nor is it straightforward to interpret all the parameters of these types of models [*Lutz et al.*, 1996]. More recently, models have been developed that express absorption spectra of phytoplankton as the sum of absorptions by two component populations [*Sathyendranath et al.*, 2001; *Ciotti et al.*, 2002]. These models are based on the conceptual model of *Yentsch and Phinney* [1989], who suggested that a background population of small, optically active phytoplankton cells is always present in oceanic waters, on which a variable population of large phytoplankton cells might be superimposed sporadically. Of these two models, the *Ciotti et al.* [2002] model does not attempt to predict phytoplankton absorption as a function of chlorophyll-*a*. As for the model of *Sathyendranath et al.* [2001], some of the difficulties with the interpretation of the parameters remained.

[4] In this paper, we extend and apply the *Sathyendranath et al.* [2001] model of phytoplankton absorption. We show that the model can be used to derive the specific absorption spectra (absorption coefficient per unit concentration of chlorophyll-*a*) of the two component populations of the phytoplankton assemblage and that the bio-optical interpre-

[1]Department of Oceanography, Dalhousie University, Halifax, Nova Scotia, Canada.
[2]Ocean Science Division, Bedford Institute of Oceanography, Dartmouth, Nova Scotia, Canada.
[3]Departamento de Oceanografia, Universidad de Concepcìon, Concepciòn, Chile.

0148-0227/06/2005JC002880

tation of the model parameters can be improved. Furthermore, the model is able to predict phytoplankton absorption as a function of chlorophyll-*a* concentration. The extended model is compared with the previously published models of *Bricaud et al.* [1995, 2004] and *Ciotti et al.* [2002]. In addition, information on the phytoplankton size structure, inferred from the values of the phytoplankton specific absorption coefficients, is compared with size classes estimated using pigment data [*Vidussi et al.*, 2001]. Because the specific absorption spectra of component phytoplankton populations can be related to the size and type of the populations, the model can be used as a bio-optical tool to explore the biogeography of phytoplankton populations. This important application of the model is demonstrated using our extensive database of phytoplankton absorption spectra to examine regional and seasonal differences in the optical characteristics of phytoplankton populations.

2. Materials and Method

2.1. Model Development

[5] In this section, we extend the model of *Sathyendranath et al.* [2001] to improve the interpretation of the model parameters. In this model, we assume that the total chlorophyll-*a* concentration (C) is the sum of the concentrations C_1 and C_2 of two phytoplankton populations 1 and 2 with distinct optical characteristics, such that

$$C = C_1 + C_2. \tag{1}$$

Of course, this is a simplification of reality, but it will be shown that the optical properties of natural phytoplankton assemblages can be described very well by combining the optical properties of the two populations in varying proportions. We assumed that C_1 is the dominant component of the phytoplankton population at low chlorophyll-*a* concentrations, and that this population does not increase to concentrations greater than some threshold value beyond which the second population becomes dominant [see *Yentsch and Phinney*, 1989]. The change in C_1, as total chlorophyll-*a* concentration C increases, is represented here as

$$C_1 = C_1^m[1 - \exp(-SC)], \tag{2}$$

such that the concentration C_1 reaches a maximum value of C_1^m asymptotically as C increases, and the initial slope S determines the rate at which C_1 increases with increase in C.

[6] Because the phytoplankton absorption coefficient is an additive property, we have

$$a_p(\lambda) = a_1^*(\lambda)C_1 + a_2^*(\lambda)C_2, \tag{3}$$

where $a_p(\lambda)$ is the total absorption coefficient due to phytoplankton at wavelength λ, and $a_1^*(\lambda)$ and $a_2^*(\lambda)$ are the specific absorption coefficients of populations 1 and 2 at λ. Combining equation (3) with equations (1) and (2), we have

$$a_p(\lambda) = C_1^m[a_1^*(\lambda) - a_2^*(\lambda)][1 - \exp(-SC)] + a_2^*(\lambda)C\,. \tag{4}$$

Sathyendranath et al. [2001] set

$$U = C_1^m[a_1^*(\lambda) - a_2^*(\lambda)], \tag{5}$$

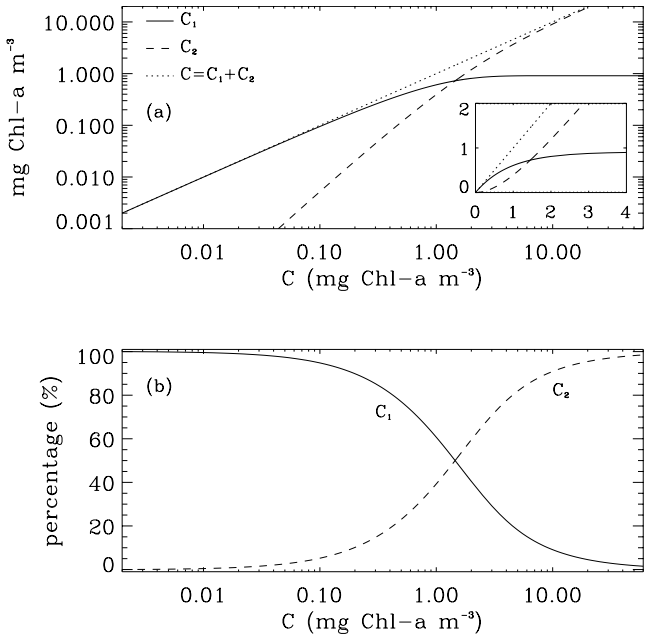

Figure 1. (a) Illustration of changes in chlorophyll concentrations C_1 and C_2 in the model as a function of the total chlorophyll-*a* concentration C for an arbitrary set of parameters. The one-to-one line $C = C_1 + C_2$ is also shown. Inset is the same variables plotted on a linear scale. (b) Percentages of C_1 and C_2 in C. Note that C_1 dominates at low concentrations and C_2 dominates at high concentrations.

where U is an unknown parameter, such that equation (4) becomes

$$a_p(\lambda) = U[1 - \exp(-SC)] + a_2^*(\lambda)C. \tag{6}$$

The parameters U, S and a_2^* are treated as unknown parameters when equation (6) is fitted by the least square method to data on phytoplankton absorption and chlorophyll-*a* concentration. *Sathyendranath et al.* [2001] pointed out that a limitation of the approach was that it is not easy to interpret U, which is a composite parameter, being a function of C_1^m, a_1^* and a_2^*. Here, we extend the model, and demonstrate how it can be used to derive the coefficients a_1^* and C_1^m, in addition to S and a_2^*. For this, we make use of the properties of the model that C_1 dominates the total population when C is small, and C_2 becomes dominant for high C (Figure 1). This allows us to solve for a_1^* and C_1^m at low C values. Once the bio-optical properties of the two populations are determined, any concentration C of chlorophyll-*a* in the medium can be expressed as the sum of concentrations C_1 and C_2, along a continuum from $C \rightarrow C_1$ at low concentrations to $C \rightarrow C_2$ at high concentrations (Figure 1).

[7] To solve for a_1^* and C_1^m, let us take the derivative of equation (6) with respect to C. We then obtain

$$\frac{da_p(\lambda)}{dC} = SU\exp(-SC) + a_2^*(\lambda). \tag{7}$$

As the concentration of C approaches 0, we obtain

$$\left.\frac{da_p(\lambda)}{dC}\right|_{C\rightarrow 0} = SU + a_2^*(\lambda). \tag{8}$$

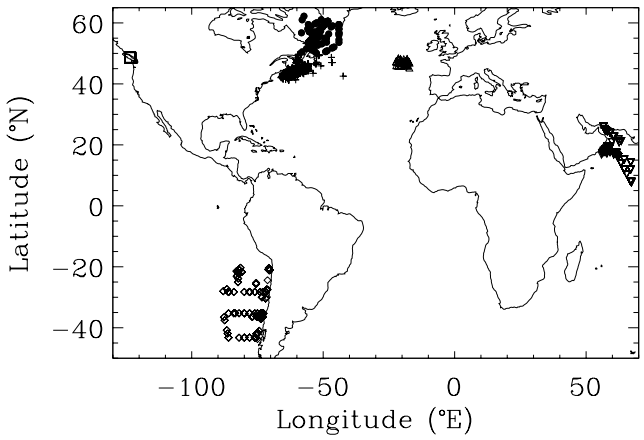

Figure 2. Locations of the stations where the phytoplankton absorption and pigment concentration data were collected. In the northwest Atlantic, the circles correspond to the latitudes higher than 50°N, and the crosses correspond to latitudes equal to or lower than 50°N. Diamonds correspond to the cruise off Chile, inverted triangles correspond to the Arabian Sea cruises, triangles correspond to the northeast Atlantic cruise, and squares correspond to the cruise off Vancouver Island. Further details about these cruises are given in Table 1.

Substituting for U from equation (5), we get

$$\left.\frac{da_p(\lambda)}{dC}\right|_{C\to 0} = S\left[C_1^m(a_1^*(\lambda) - a_2^*(\lambda))\right] + a_2^*(\lambda). \quad (9)$$

Similarly, for the slope of C_1 near the origin, let us take the derivative of equation (2) with respect to C to obtain

$$\left.\frac{dC_1}{dC}\right|_{C\to 0} = SC_1^m. \quad (10)$$

[8] When the concentration of chlorophyll-a is extremely low, the phytoplankton population is typically dominated by population 1 (Figure 1). Therefore, as C tends to zero, we make the assumption that $C_2 \to 0$, and therefore $C = C_1$. It then follows that at low concentrations, $SC_1^m = 1$. Then equation (9) reduces simply to the solution

$$\left.\frac{da_p(\lambda)}{dC}\right|_{C\to 0} = a_1^*(\lambda). \quad (11)$$

[9] Once we know $a_1^*(\lambda)$ (slope of $a_p(\lambda)$ when C tends to zero), the value of C_1^m can be obtained from equation (5) since $a_2^*(\lambda)$ is already known from fitting equation 6 to the data. Thus, by applying a single, simple and realistic assumption on the dominant phytoplankton population at low concentrations (i.e., $C_2 \to 0$ when $C \to 0$), the model of *Sathyendranath et al.* [2001] can be used to obtain information on the spectral absorption characteristics of the two dominant phytoplankton populations as well as on the asymptotic maximum concentrations attained by the population 1. Furthermore, the model can be used to estimate the fraction F of population 1 in the sample, if we know the total concentration, C. Because $F = C_1/C$, we have from equation (2)

$$F = \frac{C_1^m}{C}(1 - \exp(-SC)), \quad (12)$$

where the F parameter is expressed as a function of C, the chlorophyll-a concentration, C_1^m, the upper limit of concentration of population 1, and S, the exponential increase of C_1 with C. Note that F has a range from 0 (population 2 dominated samples) to 1 (population 1 dominated). The model as formulated does not make any a priori assumption regarding the types of phytoplankton cells that constitute populations 1 and 2. However, the model yields the specific absorption coefficients of the two populations, which in turn is used to draw conclusions about the cell sizes of the two component populations.

2.2. Other Models of Phytoplankton Absorption

[10] For comparisons with the above model, existing models of phytoplankton absorption are reformulated here. The *Bricaud et al.* [1995, 2004] model is restated here in terms of phytoplankton absorption (equation (13)) rather than specific absorption to facilitate comparison with our model:

$$a_p(\lambda) = A_1 C^{(1-B_1)}, \quad (13)$$

where A_1 and B_1 are the parameters reported by *Bricaud et al.* [1995, 2004] at any wavelength λ. Note that parameters A_1 and B_1 are available only at 440 nm from *Bricaud et al.* [2004].

[11] *Ciotti et al.* [2002] reconstructed the specific absorption spectra of phytoplankton communities as a linear combination of absorption spectra of small cells and large cells. To allow comparison with our model, their equation (3) is expressed below in terms of the specific absorption coefficients from their Table 3 (after conversion of normalized absorption spectra to specific absorption spectra using their conversion factors):

$$a_p^*(\lambda) = Fa_{\text{pico}}^*(\lambda) + (1-F)a_{\text{micro}}^*(\lambda), \quad (14)$$

where a_{pico}^* and a_{micro}^* are phytoplankton specific absorption coefficients from *Ciotti et al.* [2002] for small cells (picoplankton) and large cells (microplankton) respectively, and F represents the contribution of picoplankton (small cells) to the total absorption. (Note that the parameter F has notation $S_{\langle f \rangle}$ of *Ciotti et al.* [2002]. We have used the notation F here to avoid confusion with the parameter S in our model.)

2.3. Analysis of Samples

[12] Our model is applied to data from various regions of the world ocean. The data were collected from six regions during 34 cruises between 1994 and 2002 (Figure 2) and were grouped according to season when sufficient data were available to study seasonal variations in bio-optical properties (Table 1). Some 901 samples were used in this analysis. In the Northwest Atlantic Zone (NWAZ), the limit between high and intermediate latitudes was set at 50° N, as by *Sathyendranath et al.* [2001] to facilitate comparisons. The

Table 1. Description of the Data Set[a]

Area	Season	Year(s)	Month(s)	N
Arabian Sea	intermonsoon	1994	Nov–Dec	92
Arabian Sea	SW monsoon	1994	Aug–Sep	63
Arabian Sea	SW monsoon	1997	Jun–Jul	155
Off Chile	austral fall	1995, 1999, 2000 and 2002	Feb–Jun	19
Off Chile	austral spring	1998	Oct	114
NWA high latitudes	spring	1996 to 2002	Mar–May	68
NWA high latitudes	summer	1997 to 2002	Jun–Aug	79
NWA high latitudes	fall	1996 to 2002	Sep–Nov	22
NWA intermediate latitudes	spring	1997 to 2002	Sep–Nov	130
NWA intermediate latitudes	summer	1997 to 2002	Jun–Aug	23
NWA intermediate latitudes	fall	1997 to 2002	Mar–May	298
Northeast Atlantic	fall	1996	Sep–Oct	29
Off Vancouver Island	spring	1996	Mar	27

[a]Geographic area, season, year, month and number of data points used in this study are given. Only samples with more than five pigments (including chlorophyll-*a*) were used in the data set.

type of waters studied ranged from oligotrophic waters with small cells and low chlorophyll concentrations (northeast Atlantic, with a maximum concentration of 0.5 mg m^{-3}) to eutrophic waters with large cells and high chlorophyll concentrations (off Vancouver Island, with a maximum chlorophyll concentration of 28 mg m^{-3}).

[13] Water samples were collected on GF/F glass fiber filters, which were frozen on board in liquid nitrogen (−70° C), and returned to the laboratory for analysis. Phytoplankton absorption measurements were performed using the filter technique of *Yentsch* [1962] as modified by *Mitchell and Kiefer* [1984] [see also *Stuart et al.*, 1998; *Sathyendranath et al.*, 1999]. Absorption of total particulate matter was measured using a Shimadzu UV-2101 spectrophotometer equipped with an integrating sphere at 1 nm resolution. Absorption by detrital material was estimated using the method of *Kishino et al.* [1985] after extraction of the pigments using hot methanol. Phytoplankton absorption was obtained by subtracting the detrital component from the total particulate absorption.

[14] Pigment concentrations were measured using High Performance Liquid Chromatography (HPLC) as described by *Head and Horne* [1993]. Pigments were extracted from the frozen filters by homogenizing in 90% acetone. The pigments were identified according to their retention times and by comparison with known standards. A model II linear regression of the log-transformed HPLC data on log-transformed Turner fluorometer data [*Holm-Hansen et al.*, 1965] from the same samples explained 90% of the variance in pigments (p value < 0.01). Note that in what follows, chlorophyll-*a* refers to the sum of chlorophyll-*a*, divinyl chlorophyll-*a*, chlorophyllide-*a* and allomers and epimers as determined by HPLC analysis. We did not include phaeopigments in this analysis.

2.4. Data Analysis

[15] Where sufficient data were available (high and intermediate latitude zones of the NWAZ, the Arabian Sea and the southeast Pacific off Chile), the data were partitioned into seasons. However, samples from the northeast Atlantic and off Vancouver Island were only collected during a single cruise (Table 1). For each of the 13 subsets of data, upper and lower 5% of the specific absorption coefficients were eliminated prior to analysis, to avoid the influence of outliers. Furthermore, if the material on the filter was insufficient to quantify five or more pigments, those samples were also eliminated from the analysis [*Trees et al.*, 2000]. The number of samples that remained in each subset is listed in Table 1.

[16] The model described in section 2.1 was used to describe phytoplankton absorption over the visible spectrum (400–700 nm) as a function of chlorophyll-*a* concentration (equation (4)). The three unknown parameters, S (slope of the exponential increase of C_1 as C increases), a_2^* (specific absorption of the phytoplankton population 2) and U were computed for the whole data set and for each subset listed in Table 1. The procedure adopted for analysis was as follows: The model was first fitted to data of in situ phytoplankton absorption and chlorophyll-*a* concentration using a standard nonlinear least squares method (Levenberg-Marquardt [*Press et al.*, 1992], IDL Routine MPFITFUN) over the spectral range from 400 to 490 nm. This range was chosen because the high absorption of chlorophyll-*a* at these wavelengths ensures the greatest reliability in the fit. The computed S values were then averaged (since, according to the model, S is wavelength-independent) and used as input to compute the wavelength-dependent parameters U and a_2^* over the entire spectrum (400 to 700 nm). This avoids anomalies due to the failure of the fit at low phytoplankton absorption values (especially between 550 and 620 nm). The other model parameters C_1^m and $a_1^*(\lambda)$ were then computed using equations (5) and (10). A simplex method was selected to perform the fit at this stage because it yielded higher correlation coefficients. The analysis was carried out for the global data set (all 13 subsets combined) and for each of the subsets individually.

[17] The model outputs the specific absorption coefficients of the two component populations of phytoplankton. Small phytoplankton cells have higher specific absorption coefficients than large cells, due to pigment packaging effects and changing composition of accessory pigments [*Duysens*, 1956; *Sathyendranath et al.*, 1987; *Sosik and Mitchell*, 1991; *Kirk*, 1994; *Moore et al.*, 1995; *Bricaud et al.*, 1995; *Ciotti et al.*, 2002]. Therefore, if the specific absorption coefficient of a component at 440 nm was less than 0.05 m^2 (mg Chl-*a*)$^{-1}$, we assumed that large phytoplankton (microplankton) were dominant in that population, and higher values were taken to be indicative of small phytoplankton (picoplankton and nanoplankton). Note that the choice of the threshold value of 0.05 m^2 (mg Chl-*a*)$^{-1}$ to

Table 2. Values Obtained for Parameters C_1^m, $a_1^*(440)$, and $a_2^*(440)$ for Various Seasons and Regions[a]

Area	Season	Chl-*a* Range, mg Chl-*a* m^{-3}	C_1^m, mg Chl-*a* m^{-3}	$a_1^*(440)$, m^2 (mg Chl-*a*)$^{-1}$	$a_2^*(440)$, m^2 (mg Chl-*a*)$^{-1}$	Mean Error, %	N
Total	data set	0.049–28	0.62	0.083	0.017	27.6	901
Arabian Sea	intermonsoon	0.106–1.70	0.54	0.077	0.050	16.9	92
Arabian Sea	SW monsoon 1994	0.108–2.97	0.16	0.19	0.095	14.1	63
Arabian Sea	SW monsoon 1997	0.066–4.36	1.07	0.074	0.070	25.3	155
Off Chile	austral spring	0.156–10.6	0.58	0.051	0.021	11.1	19
Off Chile	austral fall	0.049–3.55	0.44	0.127	0.060	13.4	114
NWA high latitudes	spring	0.458–13.8	1.12	0.096	0.016	18.5	68
NWA high latitudes	summer	0.202–9.09	0.83	0.069	0.047	21.3	79
NWA high latitudes	fall	0.205–1.76	0.15	0.076	0.014	10.5	22
NWA intermediate latitudes	spring	0.205–1.76	0.77	0.051	0.015	26.0	130
NWA intermediate latitudes	summer	0.141–0.880	0.38	0.115	0.042	28.3	23
NWA intermediate latitudes	fall	0.166–3.20	0.74	0.077	0.040	22.0	298
NE Atlantic	fall	0.104–0.505	0.48	0.106	0.064	11.9	29
Off Vancouver Island	spring	0.606–28	2.38	0.050	0.027	11.7	27

[a] C_1^m, asymptotic maximum concentration attained by population 1; and $a_1^*(440)$ and $a_2^*(440)$, specific absorption coefficient of phytoplankton population 1 and 2 at 440 nm. Chlorophyll-*a* ranges for the various subsets, number of samples (N), and mean errors (over all wavelengths) in model fit are also given. Note that regional analysis often reduces model error.

partition the cells into small and large categories was arbitrary. All our computations yielded specific absorption coefficients for phytoplankton population 2 that were always lower than those of population 1. Therefore, if the specific absorption coefficient of population 2 was higher than 0.05 m^2 (mg Chl-*a*)$^{-1}$ in any of the regional analyses, it implies that only small cells are present in the samples in that subset. When $a_2^*(440)$ is less than 0.05 m^2 (mg Chl-*a*)$^{-1}$ and $a_1^*(440)$ is higher than 0.05 m^2 (mg Chl-*a*)$^{-1}$, then it implies that population 2 consists of large cells and population 1 consists of small cells. In this case, the parameter F (equation 12) can be taken as a size parameter, indicating the fraction of small cells in the total population. Finally, if both $a_1^*(440)$ and $a_2^*(440)$ are less than 0.05 m^2 (mg Chl-*a*)$^{-1}$, then we take it that only large cells were present in that subset.

[18] We also implemented the method of *Vidussi et al.* [2001], which uses seven diagnostic pigments to obtain F_p, F_n and F_m, the fractions of picoplankton, nanoplankton, and microplankton in the pigment samples. Here, the picoplankton and nanoplankton were combined into a single class. This chemotaxonomic approach yields another expression for F, the fraction of small cells in a sample:

$$F = \frac{F_p + F_n}{F_p + F_n + F_m}. \tag{15}$$

As acknowledged by *Vidussi et al.* [2001], this method may sometimes yield misleading results (e.g., small diatoms would be classified as microplankton), but it provides an independent estimate of cell size, for comparison with cell sizes estimated from absorption data.

3. Results and Discussions

[19] The *Sathyendranath et al.* [2001] model was applied to the entire data set (901 data points) with phytoplankton concentration varying between 0.05 and 28 mg Chl-*a* m^{-3} and phytoplankton absorption coefficients at 440 nm ranging from 0.007 to 0.79 m^{-1}. Values of C_1^m, $a_1^*(440)$ and $a_2^*(440)$ for the 13 subsets of data studied here and for the global data set are summarized in Table 2. Specific absorption coefficients of population 1 and 2 for the global data set are presented in Table 3 for all wavelengths between 400 and 700 nm, along with the correlation coefficients obtained at each wavelength.

3.1. Comparisons With Other Phytoplankton Absorption Models

3.1.1. Model of *Bricaud et al.* [1995]

[20] The results of this model are compared with those of *Bricaud et al.* [1995] and its revised version [*Bricaud et al.*, 2004], wherein a conventional power law was used to relate phytoplankton specific absorption coefficient to chlorophyll-*a* concentration. The results for 440, 550 and 650 nm are shown in Figure 3. Parameters A_1 and B_1 were available only at 440 nm in the *Bricaud et al.* [2004] model. The agreement between both models over the range of chlorophyll-*a* concentration from 0 to 15 mg Chl-*a* m^{-3} is striking, bearing in mind the differences in the regional and temporal distribution of the two data sets (compare our Figure 2 and Table 1 and Table 1 from *Bricaud et al.* [1995]). Both models yield similar errors (Table 4) even though only our model was fitted to our data. Both models show a very good agreement at 550 and 650 nm (Figure 3). Somewhat greater differences arise at shorter wavelengths (440 nm) at low and high concentrations. However, the model of *Sathyendranath et al.* [2001] lies between the models of *Bricaud et al.* [1995, 2004] over most of the range, at this wavelength. A statistical analysis was carried out on the residuals, expressed as the difference between estimated and measured absorptions, for chlorophyll concentrations ranging between 0 and 15 mg m^{-3}. Because the residuals for all models showed a normal distribution, tests of statistical significance [*Venables and Ripley*, 1999] on the mean (Welsh *t* test) and the variance (*F* test) were used. These significance tests address the null hypothesis that the mean and the variance of the residuals were equal for all models at 440 nm. The results showed that all models have similar variances. Analysis of the residuals showed a rejection of the hypothesis that the mean of the residuals were equal (all p values are lower than 0.01). The Welch *t* test confirmed that the models of *Bricaud et al.* [1995, 2004] were both significantly different from the one presented here at 440 nm, with our model yielding absorption values that lie in between the two models of *Bricaud et al.* [1995, 2004].

Table 3. Specific Absorption Coefficients a_1^* and a_2^* Retrieved for the Entire Data Set Using the Model of *Sathyendranath et al.* [2001][a]

λ	a_1^*	a_2^*	r	λ	a_1^*	a_2^*	r	λ	a_1^*	a_2^*	r	λ	a_1^*	a_2^*	r
400	0.0575	0.0173	0.9128	402	0.0588	0.0176	0.9114	404	0.0607	0.0177	0.9095	406	0.0628	0.0179	0.9084
408	0.0652	0.0180	0.9074	410	0.0673	0.0182	0.9065	412	0.0695	0.0182	0.9050	414	0.0710	0.0184	0.9040
416	0.0724	0.0183	0.9031	418	0.0735	0.0182	0.9019	420	0.0744	0.0180	0.9008	422	0.0752	0.0179	0.9000
424	0.0757	0.0178	0.8983	426	0.0769	0.0177	0.8971	428	0.0782	0.0177	0.8957	430	0.0800	0.0177	0.8946
432	0.0817	0.0178	0.8937	434	0.0832	0.0179	0.8929	436	0.0841	0.0179	0.8921	438	0.0844	0.0178	0.8921
440	0.0839	0.0176	0.8914	442	0.0826	0.0173	0.8918	444	0.0808	0.0169	0.8920	446	0.0787	0.0166	0.8927
448	0.0765	0.0161	0.8922	450	0.0745	0.0157	0.8918	452	0.0729	0.0154	0.8911	454	0.0720	0.0151	0.8906
456	0.0713	0.0149	0.8890	458	0.0711	0.0146	0.8876	460	0.0709	0.0143	0.8861	462	0.0707	0.0140	0.8840
464	0.0704	0.0137	0.8821	466	0.0700	0.0133	0.8799	468	0.0692	0.0129	0.8778	470	0.0682	0.0124	0.8752
472	0.0670	0.0119	0.8734	474	0.0655	0.0114	0.8713	476	0.0639	0.0109	0.8697	478	0.0624	0.0104	0.8691
480	0.0607	0.0101	0.8684	482	0.0591	0.0098	0.8694	484	0.0575	0.0095	0.8700	486	0.0560	0.0093	0.8717
488	0.0543	0.0092	0.8738	490	0.0525	0.0092	0.8766	492	0.0507	0.0091	0.8797	494	0.0488	0.0090	0.8828
496	0.0467	0.0090	0.8861	498	0.0446	0.0089	0.8893	500	0.0424	0.0089	0.8927	502	0.0402	0.0089	0.8955
504	0.0383	0.0088	0.8986	506	0.0363	0.0087	0.9011	508	0.0343	0.0086	0.9035	510	0.0327	0.0086	0.9059
512	0.0310	0.0085	0.9074	514	0.0294	0.0084	0.9091	516	0.0279	0.0084	0.9109	518	0.0264	0.0083	0.9121
520	0.0249	0.0083	0.9138	522	0.0235	0.0083	0.9150	524	0.0223	0.0082	0.9159	526	0.0212	0.0081	0.9166
528	0.0199	0.0082	0.9178	530	0.0191	0.0081	0.9180	532	0.0186	0.0080	0.9191	534	0.0171	0.0079	0.9193
536	0.0163	0.0077	0.9196	538	0.0153	0.0076	0.9199	540	0.0146	0.0075	0.9201	542	0.0138	0.0073	0.9198
544	0.0130	0.0071	0.9199	546	0.0122	0.0069	0.9197	548	0.0116	0.0067	0.9196	550	0.0109	0.0064	0.9195
552	0.0101	0.0062	0.9195	554	0.0094	0.0060	0.9200	556	0.0087	0.0057	0.9209	558	0.0080	0.0055	0.9220
560	0.0075	0.0053	0.9223	562	0.0070	0.0051	0.9234	564	0.0067	0.0049	0.9246	566	0.0062	0.0049	0.9262
568	0.0057	0.0050	0.9274	570	0.0059	0.0047	0.9292	572	0.0058	0.0046	0.9309	574	0.0061	0.0045	0.9326
576	0.0062	0.0044	0.9342	578	0.0061	0.0045	0.9351	580	0.0065	0.0044	0.9371	582	0.0065	0.0045	0.9375
584	0.0068	0.0045	0.9379	586	0.0070	0.0045	0.9379	588	0.0070	0.0045	0.9371	590	0.0072	0.0044	0.9366
592	0.0072	0.0044	0.9359	594	0.0071	0.0044	0.9353	596	0.0070	0.0043	0.9347	598	0.0068	0.0042	0.9351
600	0.0066	0.0042	0.9361	602	0.0068	0.0040	0.9374	604	0.0065	0.0041	0.9385	606	0.0065	0.0041	0.9397
608	0.0067	0.0042	0.9410	610	0.0068	0.0043	0.9425	612	0.0071	0.0044	0.9430	614	0.0072	0.0046	0.9434
616	0.0076	0.0047	0.9444	618	0.0079	0.0048	0.9439	620	0.0081	0.0048	0.9439	622	0.0082	0.0050	0.9443
624	0.0084	0.0050	0.9443	626	0.0086	0.0050	0.9440	628	0.0087	0.0051	0.9441	630	0.0089	0.0052	0.9437
632	0.0092	0.0053	0.9431	634	0.0094	0.0054	0.9426	636	0.0096	0.0054	0.9422	638	0.0097	0.0055	0.9406
640	0.0099	0.0054	0.9400	642	0.0100	0.0053	0.9387	644	0.0101	0.0053	0.9368	646	0.0104	0.0051	0.9368
648	0.0104	0.0052	0.9367	650	0.0105	0.0052	0.9374	652	0.0108	0.0053	0.9381	654	0.0113	0.0056	0.9398
656	0.0121	0.0061	0.9404	658	0.0133	0.0067	0.9409	660	0.0151	0.0075	0.9408	662	0.0173	0.0085	0.9403
664	0.0200	0.0096	0.9394	666	0.0229	0.0108	0.9390	668	0.0259	0.0118	0.9373	670	0.0285	0.0126	0.9360
672	0.0303	0.0132	0.9352	674	0.0314	0.0135	0.9346	676	0.0313	0.0133	0.9337	678	0.0304	0.0128	0.9334
680	0.0283	0.0122	0.9342	682	0.0252	0.0112	0.9346	684	0.0214	0.0101	0.9366	686	0.0175	0.0088	0.9386
688	0.0137	0.0074	0.9406	690	0.0105	0.0061	0.9416	692	0.0079	0.0049	0.9422	694	0.0059	0.0039	0.9421
696	0.0045	0.0031	0.9408	698	0.0035	0.0025	0.9392	700	0.0027	0.0020	0.9358				

[a]The absorption coefficients a_1^* and a_2^* are in units of m^{-2} (mg Chl-a)$^{-1}$. The correlation coefficient r is also indicated. The parameter S associated with the absorption data is equal to 1.61.

[21] Differences between the two models are more apparent when the specific absorption coefficients and the shapes of the absorption spectra are compared. Spectral variations of specific absorption coefficients computed with both models for various chlorophyll-*a* concentrations are plotted in Figure 4a. Both models show good agreement at wavelengths greater than 550 nm, but the model of *Bricaud et al.* [1995] yields higher specific absorption coefficients at 685 nm at low chlorophyll-*a* concentrations ($\leq$0.1 mg m^{-3}). At wavelengths lower than 550 nm, differences between the two absorption models are greater. Both models show similar spectra at intermediate concentrations (Chl-*a* = 1 mg m^{-3}). At high chlorophyll-*a* concentration (Chl-*a* = 10 and 30 mg m^{-3}), the model of *Sathyendranath et al.* [2001] gives higher chlorophyll-*a* specific absorption coefficient.

[22] Phytoplankton absorption spectra are normalized to their values at 440 nm to compare their shapes in Figure 4b. Normalized spectra obtained using the *Bricaud et al.* [1995] model show a wider range of variation, with a higher blue-to-red ratio at high chlorophyll-*a* concentrations. At wavelengths below 420 nm, normalized specific absorption coefficients computed with the model of *Sathyendranath et al.* [2001] were higher than the normalized specific absorption coefficients computed using the model of *Bricaud et al.* [1995].

[23] The divergence between models at extreme values of chlorophyll-*a* concentrations is explained to some extent by the mathematical descriptions of the two models. As chlorophyll-*a* concentrations tend to zero, the specific absorption coefficient computed with the power law of the *Bricaud et al.* [1995] model tends to infinity [*Lutz et al.*, 1996], whereas the specific absorption coefficient computed with the *Sathyendranath et al.* [2001] model tends to the finite limit of a_1^*, the specific absorption of the population 1. Similarly, at very high chlorophyll-*a* concentrations, the specific absorption coefficient computed with the *Bricaud et al.* [1995] model tends to zero whereas the specific absorption coefficient computed with the *Sathyendranath et al.* [2001] model reaches its lower limit of a_2^*, the specific absorption coefficient of population 2. Because the specific absorption coefficients are constrained within a range set by the values of a_1^* and a_2^*, in the *Sathyendranath et al.* [2001] model, it is more realistic than that of *Bricaud et al.* [1995], which allows a higher variability in specific absorption spectra (Figure 4). Since the model of *Sathyendranath et al.* [2001] is built around a biological concept (presence of

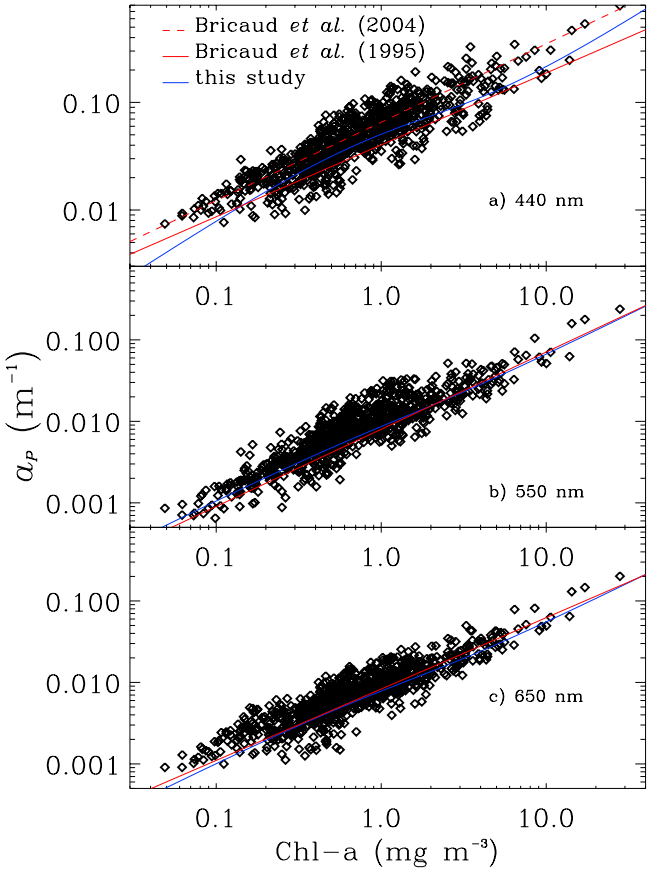

Figure 3. Phytoplankton absorption coefficients at (a) 440 nm, (b) 550 nm and (c) 650 nm versus chlorophyll-*a* concentration. Blue lines correspond to the *Sathyendranath et al.* [2001] model, red lines correspond to the *Bricaud et al.* [1995] model, and the red dashed line corresponds to the *Bricaud et al.* [2004] model.

two distinct populations each dominating at one of the extremes of chlorophyll-*a* concentrations), the parameters of the model are easily interpreted and can be used to infer some biogeographical properties of phytoplankton, as demonstrated in sections 3.2 and 3.3. The parameters of the power law model, on the other hand, are not easily interpreted, or justified, especially at the limits.

3.1.2. Model of *Ciotti et al.* [2002]

[24] Specific absorption spectra for small and large cells from the *Ciotti et al.* [2002] model (derived from the basis vectors in Table 3 of *Ciotti et al.* [2002]) and our model are comparable (Figure 5), though our model yields slightly higher specific absorption coefficients at most wavelengths.

Table 4. Root-Mean-Square Error for the Models Presented in This Paper[a]

	Bricaud et al. [1995]	Our Model
440 nm	30.4	28.0
550 nm	30.7	28.9
650 nm	31.7	28.3
400–700 nm	29.3	27.6

[a]The error is given in %. The error at 440 nm computed for the *Bricaud et al.* [2004] model is 31.7%.

The data set used here includes samples collected in very oligotrophic, tropical waters, which could explain the high chlorophyll-specific absorptions for small cells that are obtained here. The smaller specific absorption coefficient for large cells obtained by *Ciotti et al.* [2002] may be representative of data collected during intense diatom blooms in the Bedford Basin (see *Ciotti et al.*'s [2002] Table 2 with chlorophyll-*a* concentrations up to 135 mg m^{-3}).

[25] In Figure 6a, the size parameter F is plotted against the average specific absorption coefficient (computed between 400 and 700 nm). The average specific absorption for the two populations (small and large cells) is higher in the model of *Sathyendranath et al.* [2001] when applied to our global data set than in the model of *Ciotti et al.* [2002], as seen previously (Figure 5). However, some of the data from *Ciotti et al.* [2002] lie closer to the *Sathyendranath et al.* [2001] model than to the *Ciotti et al.* [2002] model (Figure 6a).

[26] In Figure 6b, the parameter F is plotted against the chlorophyll-*a* concentration for the global data set. The ranges of chlorophyll-*a* concentrations from Table 2 of *Ciotti et al.* [2002] and the corresponding F values are also shown in Figure 6b. We note that some of the *Ciotti et al.* [2002] observations are consistent with the global model presented here. However, most of the Bedford Basin data have higher F values than predicted by the global model. Such discrepancies are not surprising, considering that the Bedford Basin is a semienclosed coastal inlet. However, it is interesting to note that one set of samples from the Bering

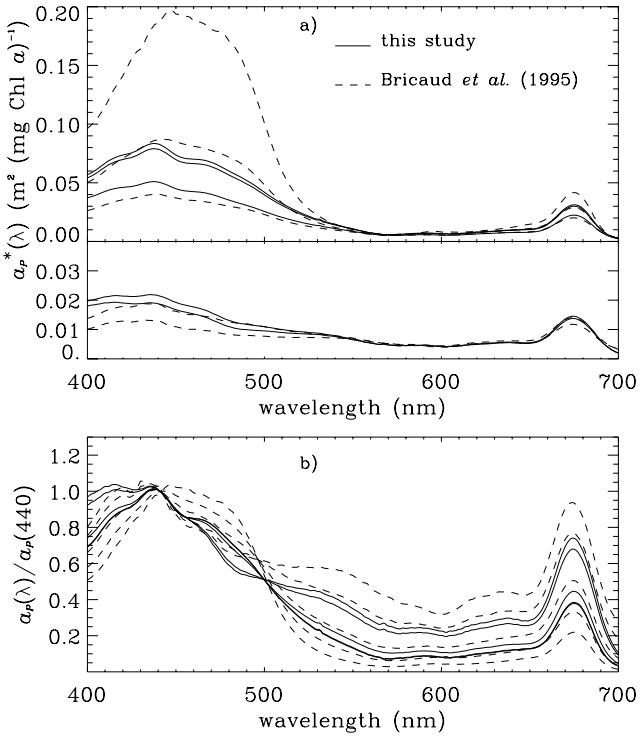

Figure 4. (a) Computed phytoplankton specific absorption spectra between 400 and 700 nm for various chlorophyll-*a* concentrations (0.01, 0.1, 1, 10 and 30 mg Chl-*a* m^{-3} from top to bottom). (b) Same spectra but normalized to $a_p^*(440)$. Solid lines correspond to the *Sathyendranath et al.* [2001] model (global data set), and dashed lines correspond to the *Bricaud et al.* [1995] model.

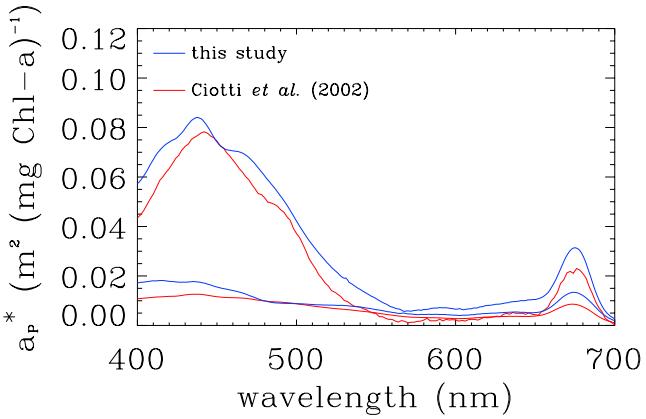

Figure 5. Small and large phytoplankton absorption spectra computed using the model of *Ciotti et al.* [2002] (red lines) and the model of *Sathyendranath et al.* [2001] applied to the global data set (blue lines).

sea also deviates significantly from the global model, highlighting possible regional and seasonal variations in the biogeography of phytoplankton. Regional variations are explored in detail in sections 3.2 and 3.3.

[27] The models of *Sathyendranath et al.* [2001] and *Ciotti et al.* [2002] are similar in that both represent total phytoplankton absorption as the sum of two components. However, the approach used by *Ciotti et al.* [2002] is different from the one used here. *Ciotti et al.* [2002] divided their samples into four classes using filtration, microscopy and fluorometry. They observed that total absorption at a given station could be reconstructed using the average absorption of the two extreme components of their classification, namely those of the microplankton and picoplankton components. In this work, the model is fitted to the whole data set of absorption coefficients and chlorophyll-*a*, assuming the presence of two populations of phytoplankton, with no a priori knowledge or assumptions about the absorption properties of either population. Furthermore, unlike the *Ciotti et al.* [2002] model, the model used here predicts how F would vary as a function of total chlorophyll-*a* concentration.

3.2. Comparison With Pigment Data

[28] Pigment composition was used to partition phytoplankton into small- and large-celled fractions following *Vidussi et al.* [2001] (as described above). The results for individual samples were averaged and are presented in Table 5. This size classification is compared here with that obtained using the two-population absorption model (Table 5). In 9 out of the 13 data sets, both the methods yield the same dominant size class. In fact, for the Arabian Sea intermonsoon season, off Vancouver Island, the northeast Atlantic, the northwest Atlantic at intermediate latitudes in summer and fall and off Chile, the two methods agree to within 15%. In the Arabian Sea SW monsoon 1994 and 1997, the dominant population identified by the absorption method is consistent with the HPLC analysis; however the percentages of large and small cells are quite different. At high latitudes in the northwest Atlantic in spring and summer, both methods yield F values close to 50%. At high latitudes in the fall, the trends are opposite. The values of F from the two methods differ most in the northwest Atlantic (intermediate latitudes) in spring, and northwest Atlantic (high latitudes) in the fall. We note, however, that the specific absorption of population 1 in the former case is very close to the threshold value of 0.05 m^2 (Chl-*a*)$^{-1}$ used to discriminate between small and large cells, which could have contributed to the mismatch with pigment data.

[29] In general, however, the absorption-based and pigment-based methods yield consistent results regarding the size structure of phytoplankton. Thus, on the basis of available data, it appears that the optical model presented here can be used to draw conclusion about the regional variability in phytoplankton size structure.

3.3. Variations in Specific Absorption Coefficient

3.3.1. Seasonal Variations

[30] The Northwest Atlantic Zone was chosen as a case study to examine seasonal differences in bio-optical properties because it was the most sampled area in our data set.

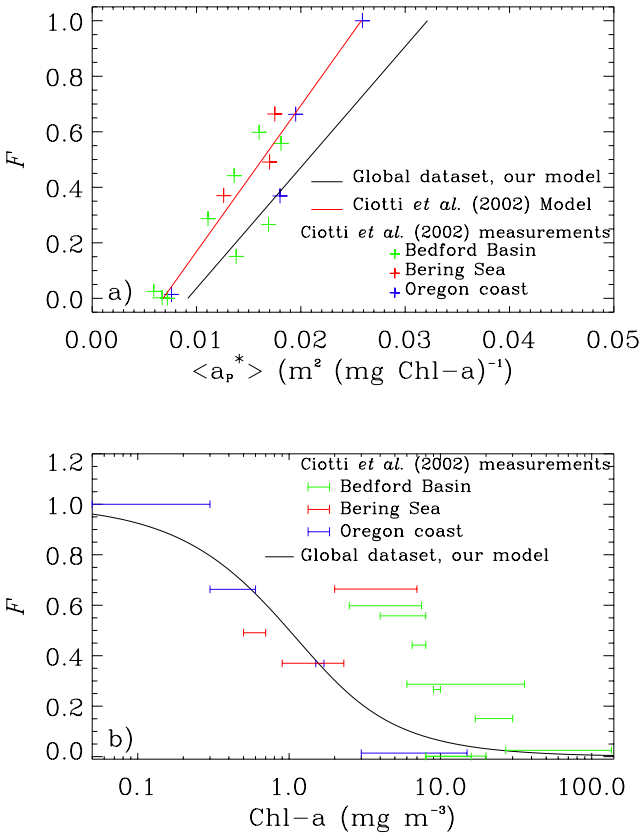

Figure 6. (a) Size parameter F computed for different phytoplankton communities by *Ciotti et al.* [2002] (crosses) and computed using our model according to equation (12) (black solid line) plotted against the mean specific absorption (averaged between 400 and 700 nm). (b) Variation of the parameter F as a function of chlorophyll-*a* concentration for the global data set (solid line). Chlorophyll-*a* concentration and F from *Ciotti et al.* [2002] observations are also indicated as horizontal bars showing the range of chlorophyll concentrations. Different colors are used in Figures 6a and 6b for the *Ciotti et al.* [2002] data to differentiate sampling locations.

Table 5. Proportion of Small and Large Phytoplankton Cells for the 13 Zones and Seasons Computed Using Pigment Data and Specific Absorption Coefficients[a]

		Phytoplankton Size Fraction, %			
		From HPLC		From Our Model	
Region	Season	F	$(1-F)$	F	$(1-F)$
Arabian Sea	intermonsoon	70.4	29.5	66.2	33.8
Arabian Sea	SW monsoon 1994	62.7	37.3	100	0
Arabian Sea	SW monsoon 1997	67.0	33.0	100	0
Off Chile	austral spring	35.7	64.3	34.3	65.7
Off Chile	austral fall	85.6	14.4	100	0
NWA high latitudes	spring	41.1	58.9	54.8	45.2
NWA high latitudes	summer	43.0	57.0	56.7	43.3
NWA high latitudes	fall	71.6	28.4	36.5	63.5
NWA int. latitudes	spring	20.6	79.4	54.4	45.6
NWA int. latitudes	summer	62.6	37.4	64.2	35.8
NWA int. latitudes	fall	68.2	31.8	61.6	38.4
NE Atlantic	fall	86.4	13.6	100	0
Off Vancouver Island	spring	7.9	92.1	0	100

[a]Note that if both $a_1^*(440)$ and $a_2^*(440)$ were less than the threshold value of 0.05 m^{-2} (mg Chl-a)$^{-1}$, then we have set $F = 0$. If the two specific absorption coefficients were greater than the threshold value, then $F = 100$. Other values of F are mean values (equation (12)) for each subset of the global data set.

A detailed analysis for spring, summer and fall for intermediate latitudes is presented here.

[31] At intermediate latitudes, the model applied to spring data differs from those of the other two seasons and the global model (Figure 7). A model II linear regression on the log-transformed spring absorption data showed a slope of 1.02 (95% confidence interval ranges between 0.92 and 1.13) and an intercept of −0.20 (95% confidence interval ranges between −0.33 and −0.08) if the summer model were used indicating that the use of summer model on spring data would introduce a systematic bias in estimated values. Absorption coefficients from summer and fall overlap, whereas lower absorption values were obtained during spring for the same chlorophyll-*a* concentrations. Lower absorption coefficients suggest that large cells are present in the spring bloom. Note that the use of the global model in the intermediate latitudes of the northwest Atlantic would result in systematic biases, and that the biases would not be the same for all seasons: the global algorithm would systematically overestimate absorption in the spring season, and underestimate absorption at all concentrations in summer and at high concentrations in the fall. These results highlight the need for seasonal and regional observations of phytoplankton absorption, since differences in specific absorption spectra have important implications for remote-sensing algorithms for interpretation of ocean color data [*Sathyendranath et al.*, 2001; *Devred et al.*, 2005].

3.3.2. Regional Variations

[32] The specific absorption spectra obtained for each area and season for the smaller size classes (based on absorption coefficients) are plotted in Figure 8a, whereas the larger size classes are shown in Figure 8b. In the Arabian Sea monsoon season (1994 and 1997), Chile austral fall and the Northeast Atlantic Zone, only small cells were sampled. In the southwest monsoon season in 1994, the Arabian Sea exhibits the highest absorption coefficients of the data presented here. It was only the intermonsoon data set from the Arabian Sea that showed the presence of large cells according to the criterion used here ($a_2^*(440) < 0.05$ m^2 (mg Chl-a)$^{-1}$). In fact, cyanobacteria (*Synechococcus* sp.) and prymnesiophytes were identified using microscopy [*Burkill et al.*, 1993; *Tarran et al.*, 1999] and pigment data [*Bidigare et al.*, 1997; *Latasa and Bidigare*, 1998] during the intermonsoon season in the Arabian Sea. Presumably, it is the prymnesiophytes that contribute to the large-cell fraction. In the northwest Atlantic, low absorption coefficients during spring at intermediate and high latitudes are seen. This is consistent with diatom blooms that are known to occur at this time of the year in the northwest Atlantic [*Stuart et al.*, 1998]. In summer, flat absorption spectra are observed only at high latitudes, suggesting a northward progression of the diatom blooms. Off the Chile coast in austral spring, the analyses of absorption coefficients reveal the presence of small and large cells in agreement with *Stuart et al.* [2004], unlike those for the austral fall where only small cells are present. The specific absorption coefficient of large cells at 440 nm is similar to the specific absorption coefficient at 440 nm measured by *Montecino et al.* [2004] in this area at the same time of the year. The Vancouver cruise shows low absorption values of microplankton, consistent with the work of *Stuart et al.* [1998], who identified diatoms in this area at the same time as the absorption measurements. In the northeast Atlantic, the phytoplankton absorption analysis indicates the presence of small phytoplankton, which is expected in these oligotrophic waters.

[33] *Yentsch and Phinney* [1989] postulated that a permanent population of optically active small cells occurs in all regions of the oceans, in addition to which a population of larger cells with different absorption characteristics would occur on shorter time scales (e.g., during blooms). The optical analysis presented here identifies the presence of small cells in almost all cases, except for the data off Vancouver Island. In the Vancouver data, the signal from small cells, if present, is masked by the strong signal from

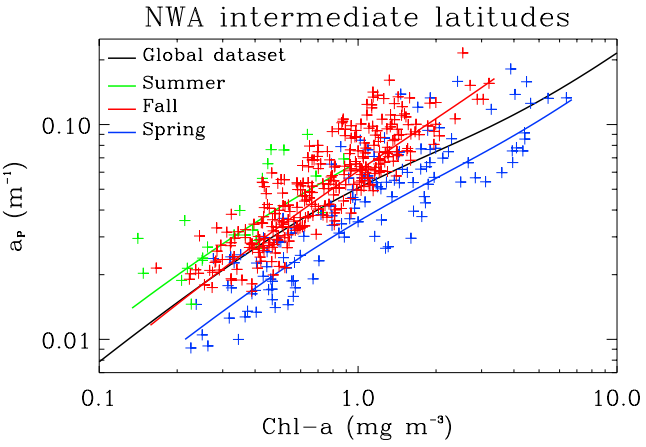

Figure 7. Chlorophyll absorption coefficient at 440 nm plotted against chlorophyll-*a* concentration. Comparison of the global model (black solid line) with the seasonal northwest Atlantic models for intermediate latitudes: spring (blue), summer (green), and fall (red).

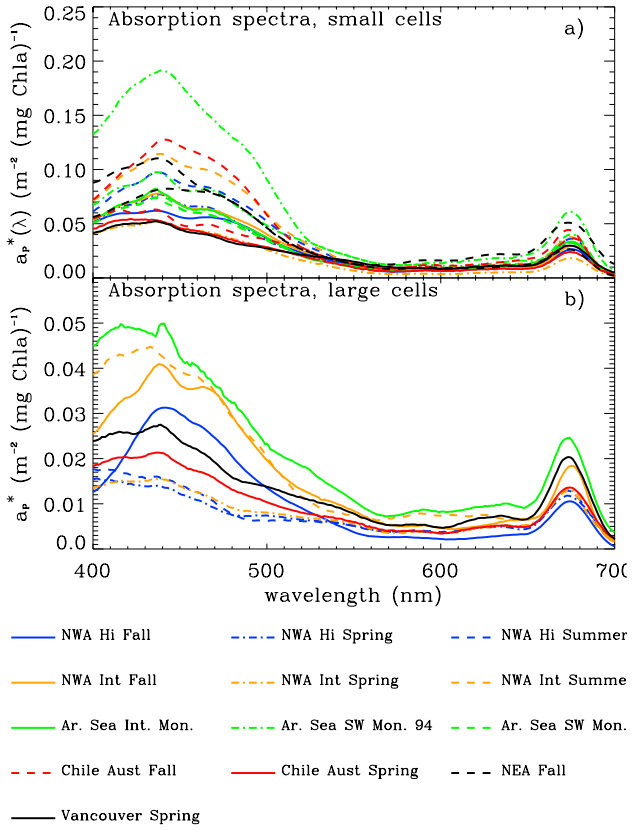

Figure 8. Phytoplankton specific absorption spectra for the study areas (see Table 1) according to phytoplankton size class: (a) small cells and (b) large cells.

diatoms: the model identifies the presence of two populations, both of large cells, suggesting that during a strong diatom bloom, absorption by small cells could become insignificant. The optical evidence presented here suggests that the hypothesis of *Yentsch and Phinney* [1989] should not be interpreted to mean that the small cells present will have uniform optical characteristics, regardless of location and season. Our results indicate that there can be significant differences in the optical characteristics of small phytoplankton with region and time, reflecting the biogeography of phytoplankton. In fact, we note a variation of a factor of two in the specific absorption of small cells at 440 nm with region. Here, we have treated picoplankton and nanophytoplankton as ''small'' cells. Interestingly, it has been reported, based on flow cytometry [*Li*, 2002] and HPLC data [*Bouman et al.*, 2005] that the relative concentrations of picoplankton and nanoplankton change, as total concentration of chlorophyll-*a* changes. Such changes in the small population could explain the optical variability of this fraction, as observed here.

[34] Knowledge of local variations in absorption characteristics can be useful for development of local algorithms to retrieve the chlorophyll-*a* concentration from ocean color [see *Sathyendranath et al.*, 2001; *Devred et al.*, 2005]. *Subramaniam et al.* [1999], *Kirkpatrick et al.* [2000] and *Sathyendranath et al.* [2004] have also pointed out the possibility of phytoplankton species identification using particular features of the absorption spectra of some phytoplankton species. Such identifications have to rely on sound knowledge of regional variability in the optical characteristics of phytoplankton.

4. Conclusion

[35] In this paper we have extended and applied the two-population absorption model of *Sathyendranath et al.* [2001]. This model assumes that large cells dominate at high chlorophyll-*a* concentrations and small cells dominate at low concentrations.

[36] The results from the model of *Sathyendranath et al.* [2001] are consistent with, and extend, the absorption models of *Bricaud et al.* [1995] and *Ciotti et al.* [2002]. It is noteworthy that the three phytoplankton absorption models discussed here have been developed using different mathematical approaches and different data sets, yet they all yield similar results. The models of *Sathyendranath et al.* [2001] and *Bricaud et al.* [1995] diverge more from each other at extreme concentrations of chlorophyll. Some of these differences arise from differences in the database, which are most pronounced at extreme pigment concentrations. However, the influence of the structure of the models on the results cannot be ruled out. As noted earlier, the *Sathyendranath et al.* model is constrained to converge on fixed values of specific absorption coefficients at low and high pigment concentrations, whereas the *Bricaud et al.* [1995] model is such that the specific absorption coefficients will tend to zero and infinity at extreme concentrations of chlorophyll. The models of *Ciotti et al.* [2002] and *Sathyendranath et al.* [2001] differ from the model of *Bricaud et al.* [1995] in the sense that they are based on the assumption that the absorption spectrum of each phytoplankton sample from natural waters can be expressed as the sum of two component spectra, representing two types of phytoplankton populations. Furthermore, the *Sathyendranath et al.* [2001] model predicts how the relative concentrations of these populations change, with change in pigment concentrations. The *Ciotti et al.* [2002] model, on the other hand, makes no prediction on how the specific absorption coefficients will change as pigment concentration varies. The model used here combines two useful features of the other models: it can be used to compute absorption by phytoplankton from chlorophyll-*a*, as in the *Bricaud et al.* [1995] model, and it can be used to study size structure of phytoplankton, as in the *Ciotti et al.* [2002] model.

[37] Application of the *Sathyendranath et al.* [2001] model to different regions and seasons showed differences in specific absorption coefficients of the two phytoplankton components, which could in turn have implications for the regional biogeochemistry of the ocean. These regional characteristics can be used to optimize regional algorithms for interpretation of ocean color data. The two-population absorption model appears to be a useful tool to identify size classes (large and small) of phytoplankton. Information on the size of the cells also has the potential to be used in modeling the backscattering properties of the phytoplankton, which is an important variable in remote sensing of ocean color.

[38] **Acknowledgments.** This work was carried out as part of the Canadian SOLAS project. This work was also supported by the Canadian Space Agency and the Department of Fisheries and Oceans, Canada. O. Ulloa was supported by the Chilean National Commission for Scientific and Technological Research (CONICYT) through the FONDAP program.

References

Bidigare, R. R., M. Latasa, Z. Johnson, R. T. Barber, C. C. Trees, and W. M. Balch (1997), Observation of a Synechococcus-dominated cyclonic eddy in open-oceanic waters of the Arabian Sea, *Proc. SPIE Ocean Opt. XIII*, *2963*, 260–265.

Bouman, H., T. Platt, S. Sathyendranath, and V. Stuart (2005), Dependence of light-saturated photosynthesis on temperature and community structure, *Deep Sea Res., Part I*, *52*(7), 1284–1299, doi:10.1016/j.dsr.2005.01.008.

Bricaud, A., M. Babin, A. Morel, and H. Claustre (1995), Variability in the chlorophyll-specific absorption coefficients of natural phytoplankton: Analysis and parameterization, *J. Geophys. Res.*, *100*, 13,321–13,332.

Bricaud, A., A. Morel, M. Babin, K. Allali, and H. Claustre (1998), Variations of light absorption by suspended particles with the chlorophyll a concentration in oceanic (case 1) waters: Analysis and implications for bio-optical models, *J. Geophys. Res.*, *103*, 31,033–31,044.

Bricaud, A., H. Claustre, J. Ras, and K. Oubelkheir (2004), Natural variability of phytoplanktonic absorption in oceanic waters: Influence of the size structure of algal population, *J. Geophys. Res.*, *109*, C11010, doi:10.1029/2004JC002419.

Burkill, P. H., R. J. G. Leakey, N. J. P. Owens, and R. F. C. Mantoura (1993), Synechococcus and its importance to the microbial foodweb of the northwestern Indian Ocean, *Deep-Sea Res.*, *40*, 773–782.

Ciotti, A. M., J. J. Cullen, and M. R. Lewis (1999), A semi-analytic model of the influence of phytoplankton community structure on the relationship between light attenuation and ocean color, *J. Geophys. Res.*, *104*, 1559–1578.

Ciotti, A. M., J. J. Cullen, and M. R. Lewis (2002), Assessment of the relationships between dominant cell size in natural phytoplankton communities and the spectral shape of absorption coefficient, *Limnol. Oceanogr.*, *47*, 404–417.

Claustre, H. (1994), The trophic status of various oceanic provinces as revealed by phytoplankton pigment signatures, *Limnol. Oceanogr.*, *39*, 1206–1210.

Cleveland, J. S. (1995), Regional models for phytoplankton absorption as a function of chlorophyll a concentration, *J. Geophys. Res.*, *100*, 13,333–13,344.

Devred, E., C. Fuentes-Yaco, S. Sathyendranath, C. Caverhill, H. Maass, V. Stuart, T. Platt, and G. White (2005), A semi-analytic, seasonal algorithm to retrieve chlorophyll-a concentration in the northwest Atlantic from SeaWiFS data, *Indian J. Mar. Sci.*, *34*(4), 356–367.

Duysens, L. M. N. (1956), The flattening of absorption spectrum of suspensions, as compared to that of solutions, *Biochim. Biophys. Acta.*, *19*, 1–12.

Fujiki, T., and S. Taguchi (2002), Variability in chlorophyll a specific absorption coefficient in marine phytoplankton as a function of cell size and irradiance, *J. Plankton Res.*, *24*, 859–874.

Head, E. J. H., and E. P. W. Horne (1993), Pigment transformation and vertical flux in an area of convergence in the North Atlantic, *Deep-Sea Res., Part II*, *40*, 329–346.

Hoepffner, N., and S. Sathyendranath (1991), Effect of pigment composition on absorption properties of phytoplankton, *Mar. Ecol. Prog. Ser.*, *73*, 11–23.

Hoepffner, N., and S. Sathyendranath (1992), Bio-optical characteristics of coastal waters: Absorption spectra of phytoplankton and pigment distribution in the western North Atlantic, *Limnol. Oceanogr.*, *37*, 1660–1679.

Hoepffner, N., and S. Sathyendranath (1993), Determination of the major groups of phytoplankton pigments from the absorption spectra of total particulate matter, *J. Geophys. Res.*, *98*, 22,789–22,803.

Holm-Hansen, O., C. J. Lorenzen, and J. D. H. Holmes (1965), Fluorometric determination of chlorophyll, *J. Cons. Cons. Int. Explor. Mer.*, *30*, 3–15.

Kirk, J. T. O. (1994), in *Light and Photosynthesis in Aquatic Ecosystems*, 3nd ed., 509 pp., Cambridge Univ. Press, New York.

Kirkpatrick, G. J., D. F. Millie, M. A. Moline, and O. Schofield (2000), Optical discrimination of a phytoplankton species in natural mixed populations, *Limnol. Oceanogr.*, *45*, 467–471.

Kishino, M., M. Takahashi, N. Okami, and S. Ichimura (1985), Estimation of the spectral absorption coefficients of phytoplankton in the sea, *Bull. Mar. Sci.*, *37*, 634–642.

Latasa, M., and R. R. Bidigare (1998), A comparison of phytoplankton populations of the Arabian Sea during the Spring Intermonsoon and Southwest Monsoon of 1995 as described by HPLC-analysed pigments, *Deep Sea Res., Part II*, *45*, 2133–2170.

Li, W. K. W. (2002), Macroecological patterns of phytoplankton in northwestern North Atlantic, *Nature*, *419*, 154–157.

Lohrenz, S. E., A. D. Weidemann, and M. Tuel (2003), Phytoplankton spectral absorption as influenced by community size structure and pigment composition, *J. Plankton Res.*, *25*, 35–61.

Lutz, V. A., S. Sathyendranath, and E. J. H. Head (1996), Absorption coefficient of phytoplankton: Regional variations in the North Atlantic, *Mar. Ecol. Prog. Ser.*, *135*, 197–213.

Mitchell, B. G., and B. A. Kiefer (1984), Determination of absorption and fluorescence excitation spectra for phytoplankton, in *Marine Phytoplankton and Productivity*, edited by O. Holm-Hansen, L. Bolis, and R. Giles, pp. 157–169, Springer, New York.

Montecino, V., R. Astoreca, G. Alarcón, L. Retamal, and G. Pizarro (2004), Bio-optical characteristics and primary productivity during upwelling and non-upwelling conditions in a highly productive coastal ecosystem off central Chile (∼36°S), *Deep Sea Res., Part II*, *51*, 2413–2426.

Moore, L. R., R. Goericke, and S. W. Chisholm (1995), Comparative physiology of *Synechococcus* and *Prochlorococcus*: Influence of light and temperature on growth, pigments, fluorescence and absorptive properties, *Mar. Ecol. Prog. Ser.*, *116*, 259–275.

Morel, A. (1991), Light and marine photosynthesis: a spectral model with geochemical and climatological implications, *Prog. Oceanogr.*, *26*, 263–306.

Press, W. H., S. A. Keukolsky, W. T. Vettering, and B. P. Flannery (1992), Levenberg-Marquard Method, in *Numerical Recipes in C: The Art of Scientific Computation*, pp. 542–547, Cambridge Univ. Press, New York.

Prieur, L., and S. Sathyendranath (1981), An optical classification of coastal and oceanic waters based on the specific spectral absorption curves of phytoplankton pigments, dissolved organic matter and other particulate materials, *Limnol. Oceanogr.*, *26*, 671–689.

Sathyendranath, S., and T. Platt (1988), The spectral irradiance field at the surface and in the interior of the ocean: A model for applications in oceanography and remote sensing, *J. Geophys. Res.*, *93*, 9270–9280.

Sathyendranath, S., L. Lazzara, and L. Prieur (1987), Variation in the spectral values of specific absorption of phytoplankton, *Limnol. Oceanogr.*, *32*, 403–415.

Sathyendranath, S., V. Stuart, B. D. Irwin, H. Maass, G. Savidge, L. Gilpin, and T. Platt (1999), Seasonal variation in bio-optical properties of phytoplankton in the N.W. Indian Ocean, *Deep Sea Res., Part II*, *46*, 633–654.

Sathyendranath, S., G. Cota, V. Stuart, H. Maass, and T. Platt (2001), Remote sensing of phytoplankton pigments: A comparison of empirical and theoretical approaches, *Int. J. Remote Sens.*, *22*, 249–273.

Sathyendranath, S., L. Watts, E. Devred, T. Platt, C. Caverhill, and H. Maass (2004), Discrimination of diatoms from other phytoplankton using ocean-colour data, *Mar. Ecol. Prog. Ser.*, *272*, 59–68.

Sathyendranath, S., V. Stuart, T. Platt, H. Bouman, O. Ulloa, and H. Maass (2005), Remote sensing of ocean colour: Towards algorithms for retrieval of pigment composition, *Indian J. Mar. Sci.*, *34*, 333–340.

Sosik, H. M., and B. G. Mitchell (1991), Absorption, fluorescence and quantum yield for growth in nitrogen-limited Dunaliella tertiolecta, *Limnol. Oceanogr.*, *36*, 910–921.

Stuart, V., S. Sathyendranath, T. Platt, H. Maass, and B. D. Irwin (1998), Pigments and species composition of natural phytoplankton populations: effect on the absorption spectra, *J. Plankton Res.*, *20*, 187–217.

Stuart, V., O. Ulloa, G. Alarcón, S. Sathyendranath, H. Major, E. J. H. Head, and T. Platt (2004), Bio-optical characteristics of phytoplankton populations in the upwelling system off the coast of Chile, *Rev. Chilean Hist. Nat.*, *77*, 87–105.

Subramaniam, A., E. J. Carpenter, D. Karentz, and P. G. Falkowski (1999), Bio-optical properties of the marine diazotrophic cyanobacteria *Trichodesmium* spp. I. absorption and photosynthetic action spectra, *Limnol. Oceanogr.*, *44*, 608–617.

Tarran, G. A., P. H. Burkill, E. S. Edwards, and E. M. S. Woodward (1999), Phytoplankton community structure in the Arabian Sea during and after the SW monsoon 1994, *Deep Sea Res., Part II*, *46*, 655–676.

Trees, C. C., D. K. Clark, R. R. Bidigare, M. E. Ondrusek, and J. L. Mueller (2000), Accessory pigments versus chlorophyll a concentrations within the euphotic zone: A ubiquitous relationship, *Limnol. Oceanogr.*, *45*, 1130–1143.

Venables, W. N., and B. D. Ripley (1999), *Modern Applied Statistic With S-Plus*, 3rd ed., 501 pp., Springer, New York.

Vidussi, F., H. Claustre, B. B. Manca, A. Luchetta, and J. C. Marty (2001), Phytoplankton pigment distribution in relation to upper thermocline circulation in the eastern Mediteranean Sea during winter, *J. Geophys. Res.*, *106*, 19,939–19,956.

Yentsch, C. S. (1962), Measurement of visible light absorption by particulate matter in the ocean, *Limnol. Oceanogr.*, *7*, 207–217.

Yentsch, C. S., and D. A. Phinney (1989), A bridge between ocean optics and microbial ecology, *Limnol. Oceanogr.*, *34*, 1694–1704.

E. Devred, H. Maass, T. Platt, S. Sathyendranath, and V. Stuart, Ocean Science Division, Bedford Institute of Oceanography, Box 1006, Dartmouth, Nova Scotia, Canada B2Y 4A2. (devrede@mar.dfo-mpo.gc.ca; maassh@mar.dfo-mpo.gc.ca; tplatt@dal.ca; shubha@dal.ca; stuartv@mar.dfo-mpo.gc.ca)

O. Ulloa, Departamento de Oceanografía, Centro de Investigaciòn Oceanográfica (COPAS) Universidad de Concepcion Casilla 160-C, Correo 3 Concepciòn, Chile. (oulloa@profc.udec.cl)